View metadata, citation and similar papers at core.ac.uk

brought to you by CORE

provided by Open Archive Toulouse Archive Ouverte

Open Archive TOULOUSE Archive Ouverte (OATAO)

OATAO is an open access repository that collects the work of Toulouse researchers and makes it freely available over the web where possible.

This is an author-deposited version published in: http://oatao.univ-toulouse.fr/
Eprints ID : 20114

To link to this article: DOI: 10.1016/S0017-9310(05)80130-9
URL: http://dx.doi.org/10.1016/S0017-9310(05)80130-9

To cite this version : Duquenne, Philippe and Deltour, Alain and Lacoste, Germain *Application of inductive heating to granular media: temperature distribution in a granular bed.* (1993) International Journal of Heat and Mass Transfer, vol. 36 (n° 9). pp. 2473 -2477. ISSN 0017-9310

Any correspondence concerning this service should be sent to the repository administrator: staff-oatao@listes-diff.inp-toulouse.fr

Application of inductive heating to granular media: temperature distribution in a granular bed

P. DUQUENNE,† A. DELTOUR‡ and G. LACOSTE†

†Laboratoire de Génie Electrochimique et d'Energétique des Réacteurs, E.N.S.I.G.C., Chemin de la Loge, 31078 Toulouse Cedex, France

‡Institut de Mécanique des Fluides, E.N.S.E.E.I.H.T., 2 rue Camichel, 31071 Toulouse Cedex, France

INTRODUCTION

INDUCTIVE heating aims at creating eddy currents in a conductor material by means of a periodic electromagnetic field; these currents generate heat by the Joule effect. This method and its applications, especially in surface treatment for metallurgy, have been studied for a long time, since it provides a fast and efficient way of heating items [1, 2]. Another quality of this process is that it is all-electric, which makes it reliable, clean and easy to automate [3].

Granular media are of great importance in any process that sets transfer phenomena between a solid matrix and a fluid phase in action, since any transfer can be expressed by the product of a transfer coefficient by a contact surface and by an exchange potential difference (difference of temperature for heat transfers and concentration gradient for mass transfers). Thus, they allow important transfers even for small values of exchange potential.

Therefore, the theme of this paper is the coupling of these domains and an investigation about the way qualities of both of them could be gathered in the same process. From the application of this principle may arise a new kind of fluid heater capable of achieving a soft warming, especially attractive for the heat-fearing fluids frequently encountered in petrochemical, pharmaceutical or biochemical industries [3]. It could also be a way of regenerating efficiently activated carbons after use [4].

BEHAVIOUR CHARACTERIZATION

The first challenge of this study is to determine the way a granular bed will react when submitted to an inductive field. In the case of an homogeneous piece of a conductor material, it is well known that eddy currents develop near the piece periphery and decrease towards its core. This phenomenon is called the 'skin effect' and introduces a penetration depth such that if it is small compared with the piece dimensions, everything happens nearly as if the eddy currents were uniform within this depth near the surface and null everywhere else [5]. Penetration depth is given by

$$\delta = \sqrt{\left(\frac{\rho_e}{\pi\mu f}\right)}.$$

It means that, provided the adequate frequency can be delivered, heating effects can be restrained to a domain as reduced as desired. But it is obvious that if the skin effect can be observed at a granular bed-scale, temperature gradients will be induced and common properties of porous media no longer have any meaning.

A second hypothesis may be formulated, assuming that particle-scale skin effects are observable, and that every granule in the bed plays the same part in heat generation—that is to say, the reactor has a volumic working mode. In this case, heat transfer between the two phases can be described by a plug-flow model (conduction phenomena in both phases are supposed to be small and the only transport mechanism is due to the uniform and parallel-to-bed-axis fluid flow), or by a plug-flow-and-dispersion model, where dispersion causes a temperature redistribution in the reactor: then effective conductivities add their effects to the plug-flow transfers. We have neglected wall effects associated with the porosity variations, then we have evaluated experimental Reynolds numbers varying between 4 and 13, with the classical filtration definition in porous media

$$Re = \frac{\rho v d_h}{\mu}.$$

For these values, the plug-flow without dispersion model can be considered to be representative for heat [6] as well as mass [7] transfers. If we do take into account the axial dispersion effects, we can consider the reactor as three separate zones $D0$, $D1$ and $D2$, corresponding to the fluid inlet, the active zone where heating takes place, and the fluid outlet, respectively (Fig. 1). Transfers between the solid matrix and the fluid can then be expressed, in steady-state regime

- for $D0$:

$$(\rho C_p)_f v \frac{\partial T_f}{\partial z} = \lambda_f \frac{\partial^2 T_f}{\partial z^2}$$

- for $D1$:

$$(\rho C_p)_f v \frac{\partial T_f}{\partial z} = \lambda_f^* \frac{\partial^2 T_f}{\partial z^2} + hS_p(T_s - T_f)$$

$$0 = \lambda_s^* \frac{\partial^2 T_s}{\partial z^2} + hS_p(T_f - T_s) + p$$

for the fluid and solid phases, respectively, according to the two energy equations model with a solid/fluid convective transfer coefficient [8]:

- for $D2$:

$$(\rho C_p)_f v \frac{\partial T_f}{\partial z} = \lambda_f \frac{\partial^2 T_f}{\partial z^2}.$$

If we put

$$\theta = \frac{T_f - T_{f,e}}{T_{fL} - T_{f,e}}, \quad \text{and} \quad Z = \frac{z}{L},$$

these equations become

NOMENCLATURE

A_0, A_1	non-dimensional numbers
C_0, C_1, C_2	integration constants
C_p	heat capacity [J kg^{-1} K^{-1}]
d_b	ball diameter [m]
h	solid/fluid local transfer coefficient [W m^{-2} K^{-1}]
	instantaneous and peak currents [A]
	reactor length [m]
	power input [W]
p	volumic power input [W m^{-3}]
Re	Reynolds number
S	reactor cross-sectional area [m^2]
S_p	contact area per unit volume [m^2 m^{-3}]
T_f	fluid phase temperature [°C]
T_f	fluid initial temperature [°C]
T_{f0}	fluid inlet temperature [°C]
T_{fL}	fluid outlet temperature [°C]
T_s	solid phase temperature [°C]
U_0, U_1	non-dimensional numbers
v	fluid velocity [m s^{-1}]
V, V_p	instantaneous and peak tensions [V]
	distance from reactor entrance [m]
Z	non-dimensional distance from reactor entrance.

Greek symbols

δ	penetration depth [m]
θ	non dimensional fluid temperature
λ_f, λ_f^*	fluid phase thermal conductivity and effective [W m^{-1} K^{-1}]
λ_s^*	effective solid phase thermal conductivity [W m^{-1} K^{-1}]
μ	magnetic permeability [F m^{-1}]
ρ	density [kg m^{-3}]
ρ_e	electric resistivity [Ω m]
ϕ	diffi
ψ	bed void fraction.

• for $D0$:

$$\frac{\partial^2\theta}{\partial Z^2} = \frac{(\rho C_p)_f v L}{\lambda_f^*}\frac{\partial\theta}{\partial Z} = A_0\frac{\partial\theta}{\partial Z}$$

leading to the following equation

$$\theta_0 = \frac{U_0}{A_0}\exp(A_0 Z) + C_0.$$

For the heating zone ($D1$), we assume the heat conduction in the solid to be negligible [9–11], that is to say that, in the case of a metallic bed, the solid temperature profile is linear ($\partial T_s/\partial z$ is constant).

In that case, the fluid-phase equation becomes

$$\frac{\partial^2\theta}{\partial Z^2} - \frac{(\rho C_p)_f v L}{\lambda_f^*}\frac{\partial\theta}{\partial Z} + \frac{pL^2}{\lambda_f^*(T_{fL}-T_{f\infty})} = 0.$$

Noticing that the total power input P can be written

$$P = pSL = (\rho C_p)_f v S(T_{fL} - T_{f\infty})$$

and introducing

$$A_1 = \frac{(\rho C_p)_f v L}{\lambda_f^*},$$

we have

$$\frac{\partial^2\theta}{\partial Z^2} - A_1\frac{\partial\theta}{\partial Z} + A_1 = 0$$

leading to the expression of θ in $D1$

$$\theta_1 = Z - \frac{\exp[A_1(Z-1)]}{A_1} + C_1$$

where C_1 is an integration constant.

The last zone gives an equation similar to that of the first one, with different constants U_2 and C_2

$$\theta_2 = \frac{U_2}{A_0}\exp(A_0 Z) + C_2.$$

Boundary conditions

They can be written as follows, for continuous values of temperature and heat flux

• for $z = -\infty$ ($Z = -\infty$): $T_f = T_{f\infty}$ and $\frac{\partial T_f}{\partial z} = 0$

• for $z = 0$ ($Z = 0$), $T_{f0}(D0) = T_{f0}(D1)$ and

$$\lambda_f\frac{\partial T_f(D0)}{\partial z} = \lambda_f^*\frac{\partial T_f(D1)}{\partial z}$$

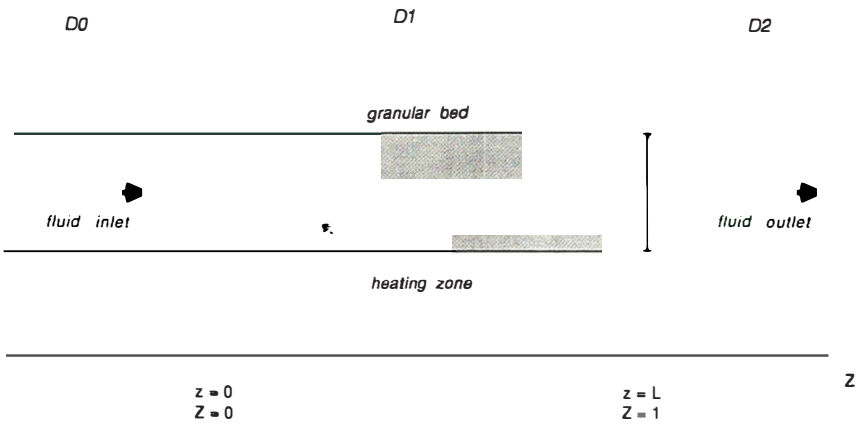

FIG. 1. Theoretical scheme of the reactor.

• for $z = L$ ($Z = 1$), $T_{f0}(D1) = T_{f0}(D2)$ and

$$\lambda_f^* \frac{\partial T_f(D1)}{\partial z} = \lambda_f \frac{\partial T_f(D2)}{\partial z}.$$

Once these conditions are introduced in the system of equations above, we have

• for $D0$:

$$\theta_0 = \frac{U_0}{A_0} \exp(A_0 Z)$$

where

$$U_0 = \frac{\lambda_f^*}{\lambda_f}[1 - \exp(-A_1)]$$

• for $D1$:

$$\theta_1 = Z + \frac{1 - \exp[A_1(Z-1)]}{A_1}$$

• for $D2$, the resolution gives $T_f = T_{fL}$.

We are now to investigate the working mode of induction-heated granular beds, and to compare experimental temperature profiles with the values given by the plug-flow with axial dispersion model.

Experimental equipment and measures

The rig (Fig. 2) is successively composed of:

• a rectifier plugged to the mains with a variable output voltage, in charge of supplying the generator;

• a generator providing crenel tension; the tension alternates between two values $+E$ and $-E$ with a frequency varying from 0 to 20 kHz. The value of E is monitored with the rectifier and can be set up to 100 V, while the current delivered can not exceed 80 peak amperes;

• a set of capacitors in charge of reducing the difference in phase between current and tension;

• an oscilloscope allowing measures of tension, current, difference in phase and frequency;

• a 195 mm-ID, 225 mm-high Plexiglas reactor circled with a 63 whorls-Litz wire inductor. Plexiglas was chosen for its infinite resistivity and thus does not modify nor stop the magnetic field. Fluid inlet is equipped with a flow meter, and a tranquillizing zone (a glass ball bed unaffected by electromagnetic induction) precedes the active zone (a steel ball bed) so that plug-flow conditions are ensured in the fluid phase;

• a Luxtron 755 optic fibre temperature probes set giving access to up to four different temperatures. This equipment is linked to a computer and can record temperature evolutions with time. The choice of optic fibre probes is dictated by the fact that classical thermocouples can easily be heated with inductive field;

• two Plexiglas tubes meant to be fitted in the reactor and part it in three concentric zones. These tubes have no influence on the magnetic field but represent a good handicap for convective as well as conductive radial heat transfers.

The measures at our disposal are temperatures profiles in the reactor; the power supplied is evaluated from integration of instantaneous values of tension and current; they can compare well with values directly calculated by the oscilloscope

$$P = \frac{V_p I_p}{2\pi} \cos(\phi)$$

where V_p and I_p are peak values of tension and current. These values also lead to the global equivalent electric resistance and inductance of the reactor and its load.

RESULTS

In the following, the reactor load is an 8 mm diameter steel ball bed percolated by water. The fluid flow, for the results presented in figures, was set at 56.6 l h^{-1} and the power input at 3600 W with a frequency of 3.75 kHz.

Working mode

In a first series of experiments, temperatures were measured for three radial positions ($r = 0$, 48 and 96 mm) at different distances from the bed entrance. Results are plotted in Fig. 3; we notice no significant difference between the core

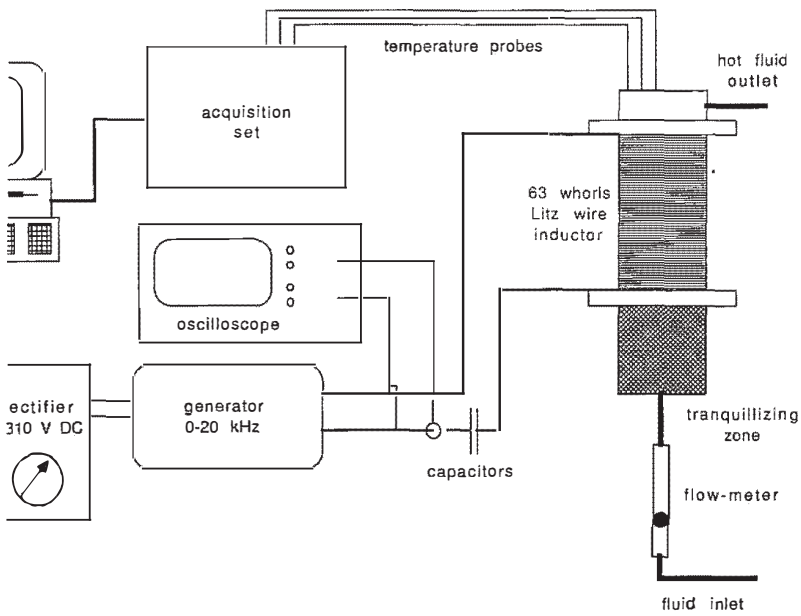

FIG. 2. Experimental apparatus.

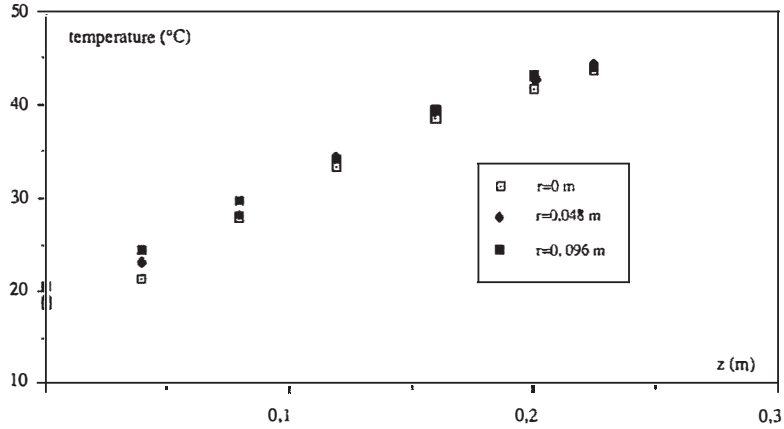

FIG. 3. Fluid temperature in the bed without concentric walls.

and the periphery of the bed. This could mean that, as expected, the energy is spread evenly in the reactor and that each of its particles has the same behaviour towards inductive heating as any other one. But this cheerful result can also be due to radial dispersion leading to a temperature homogenization in any given section of the bed.

The same measurements were performed while the reactor was equipped with the two concentric Plexiglas tubes in, with results given in Fig. 4; since Plexiglas walls in the reactor stop heat transfers whatever their nature (thermal radiation is negligible in this range of temperature), each of the three delimited zones is assumed to be independent in terms of solid/fluid transfers. The figure clearly shows that the three zones receive the same power density. Comparison between Figs. 3 and 4, which show almost the same temperature profiles within the bed for the steady-state regime, also indicates that Plexiglas walls have no influence on transport phenomena, which can be explained by weak influence of radial dispersion.

Other experiments were performed with no fluid flow through the granular bed, some using a 2 mm-high, 5 mm-diameter explorer coil plugged to the oscilloscope in order to measure local magnetic induction field at different places in the reactor, others with an 8 mm steel ball in which a thermocouple was set. They all confirm the fact that both induction and its effects are uniform in the bed.

Prediction of temperature profile

Figure 5 displays on the same graph experimental temperature profiles in the bed (without Plexiglas walls) compared with predictions given by the plug-flow with axial dispersion model. The effective fluid-phase thermal conductivity λ_f^* was set equal to $(1-\psi)\lambda_f$ [12, 13].

Experimental values at a given distance from the reactor active zone entrance are an average of the temperatures at the same distance for the three radial positions explored. As no important deviation exists between the two sets of points, we conclude that the hypothesis of a plug-flow with axial dispersion phenomena is justified.

Moreover, the temperatures profiles we have encountered throughout these experiments all show quite a good linearity, leading us to believe that the effects of axial dispersion could have been neglected [6, 7].

Efficiencies

Calculations were made to define the energetic efficiency of the inductive heater. This efficiency is the ratio of the energy transferred to the fluid phase (calculated from the fluid flow and the inlet and outlet temperatures) to that delivered by the generator, determined with the oscilloscope. Figure 6 shows this efficiency and its variations for different frequencies.

In that series of experiments, the fluid flow remains con-

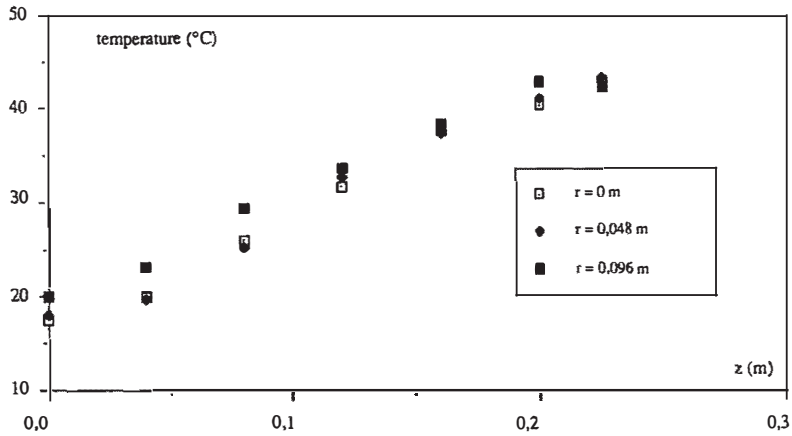

FIG. 4. Fluid temperature in the bed with concentric walls.

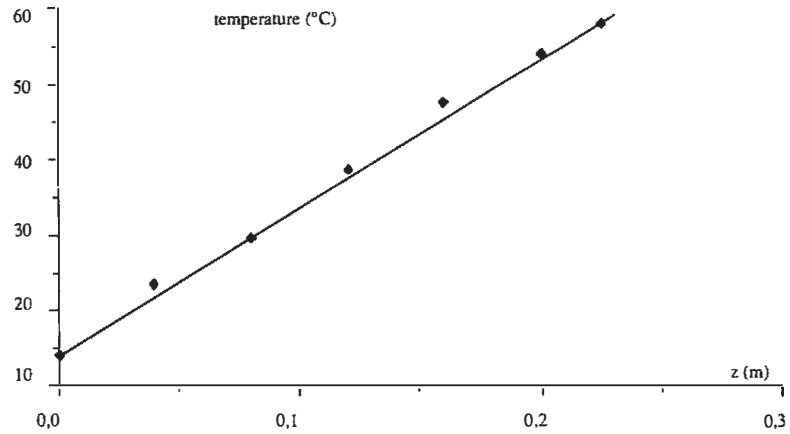

FIG. 5. Fluid-phase temperature: experiments/plug-flow with axial dispersion model comparison.

stant and the generator frequency is set to different values varying from 3 to 9 kHz. According to what is commonly observed about a homogeneous load in an inductive heater, values of efficiency are quite high and tend to rise with increasing frequencies; from 0.75 corresponding to 3 kHz, it climbs rapidly to 0.9 at 9 kHz. We can see, as for homogeneous loads [5], that there is a critical frequency beyond which it is not worth working, for an increase of this frequency provides no significant betterment of efficiency. In our case, this frequency may be estimated at about 6 or 7 kHz.

Effective thermal conductivity

One hypothesis was made, assuming that $\lambda_f^* = (1-\psi)\lambda_f$. In order to make sure of its validity, we have performed some calculations with other models predicting values of λ_f^* in packed beds [11, 12]. The result is that no influence of axial dispersion can be seen in the domain we studied, according to what can be learnt from the literature [6, 7]: this influence cannot be detected for values of λ_f^* lower than 10 W m^{-1} K^{-1}.

Thus, in the experimental domain we investigated, we can express the temperature profile in the reactor with a plug-flow without dispersion model. Assuming this, we have in steady-state conditions:

- for the fluid phase:

$$(\rho C_p)_f v \frac{dT_f}{dz} = hS_p(T_s - T_f)$$

- and for the solid:

$$0 = hS_p(T_s - T_f) + \frac{P}{SL}$$

with the following boundary condition:

$$T_f(z = 0) = T_{f0}.$$

Considering that in a steady-state regime, the whole energy input is transferred to the fluid, we are allowed to write:

$$P = (\rho C_p)_f v S(T_{fL} - T_{f0}).$$

We can then express the temperature profile according to the plug-flow model:

$$T_f(z) = \frac{T_{fL} - T_{f0}}{L} z + T_{f0}.$$

Application of experimental heat transfer coefficient evaluation

The interruption of heating may be expressed as a step method for the heat transfer evaluation. A thermal balance between the variation of the forced flow enthalpy integrated

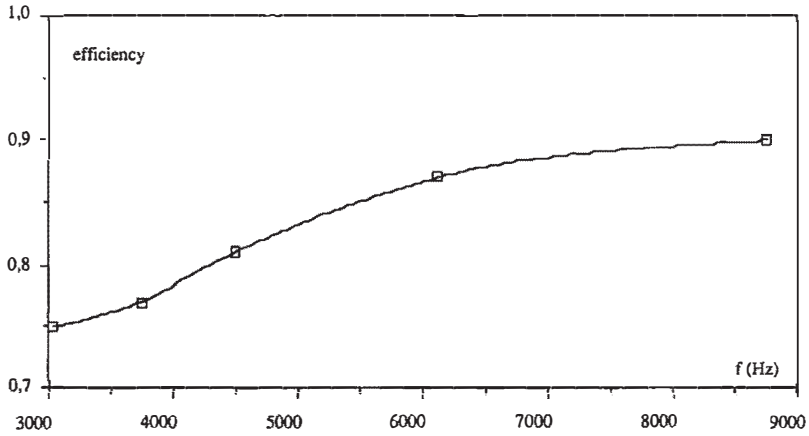

FIG. 6. Energetic efficiency: influence of frequency.